

**Cannabinoid receptor-1 signaling in hepatocytes and stellate cells does not contribute to  
NAFLD**

Simeng Wang<sup>1</sup>, Qingzhang Zhu<sup>1</sup>, Guosheng Liang<sup>1,2</sup>, Tania Franks<sup>4</sup>, Magalie Boucher<sup>4</sup>, Kendra K. Bence<sup>3</sup>, Mingjian Lu<sup>3</sup>, Carlos M. Castorena<sup>1</sup>, Shangang Zhao<sup>1</sup>, Joel K. Elmquist<sup>1</sup>, Philipp E. Scherer<sup>1</sup>, and Jay D. Horton<sup>1,2</sup>

<sup>1</sup> Department of Internal Medicine, University of Texas Southwestern Medical Center, Dallas, TX 75390-9046

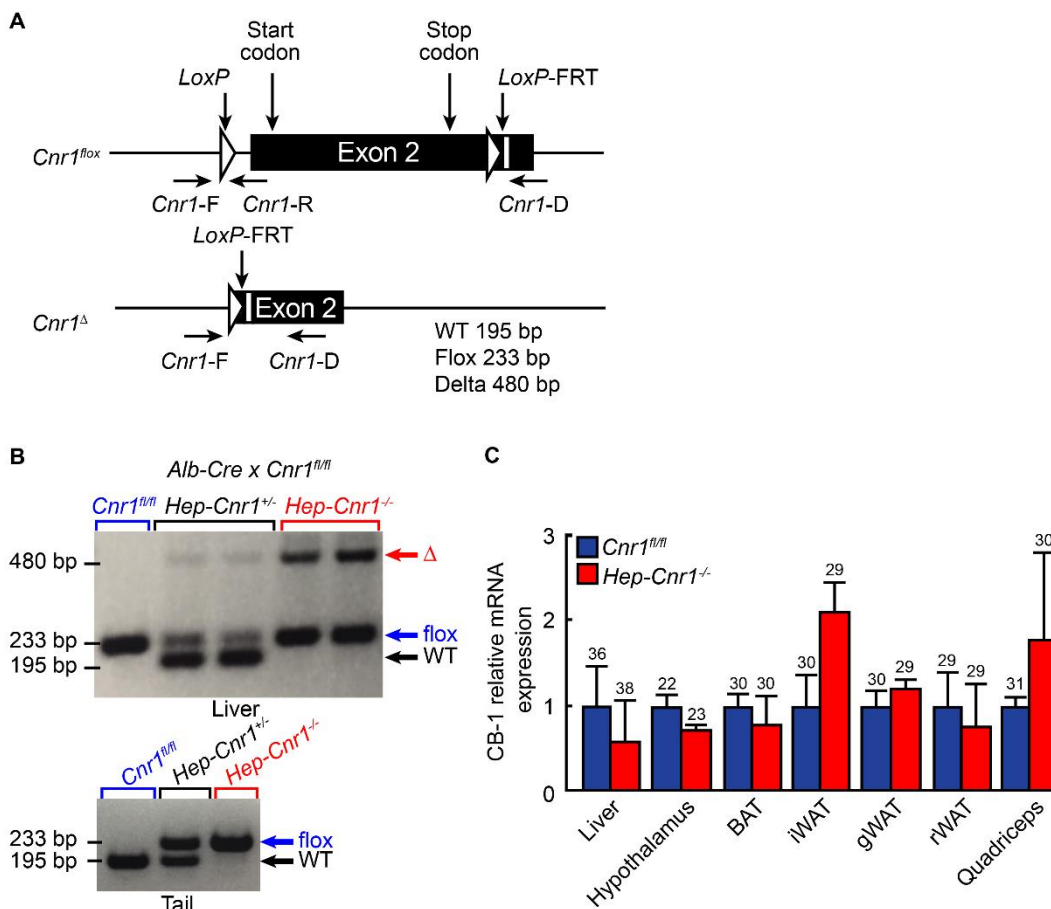
<sup>2</sup> Department of Molecular Genetics, University of Texas Southwestern Medical Center, Dallas, TX 75390-9046

<sup>3</sup> Internal Medicine Research Unit, Pfizer Worldwide Research, Development, and Medical, Cambridge, MA 02139

<sup>4</sup> Drug Safety Research and Development, Pfizer Inc, Groton CT 06340 and Cambridge, MA 02139

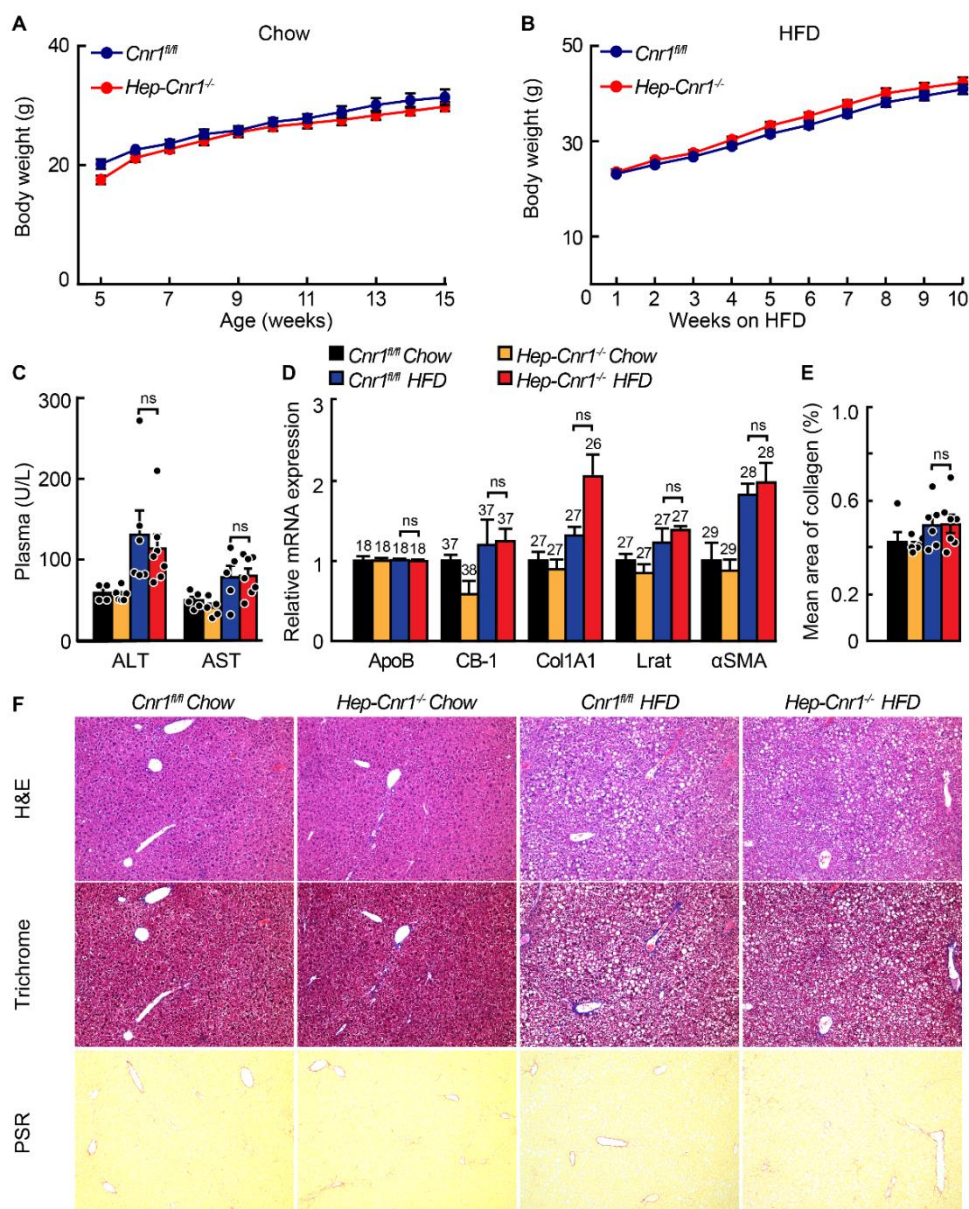
**Conflict of interest:** Jay D. Horton is on the SAB for Pfizer. Joel K. Elmquist and Guosheng Liang conduct sponsored research with Pfizer.

## Supplemental figures and figure legends



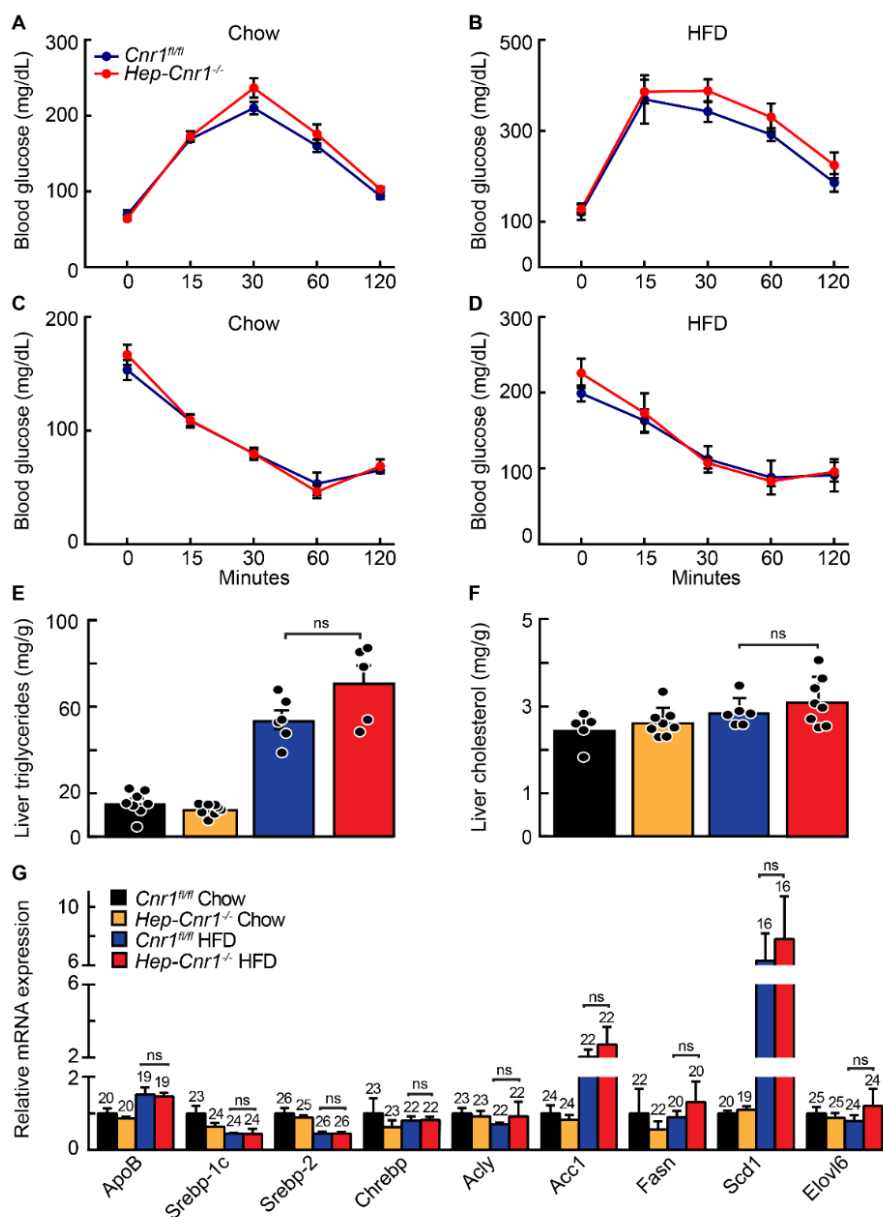
**Supplemental Figure 1. Generation and verification of hepatocyte-specific *Cnr1* knockout mice.** (A) Gene-targeting strategy for *Cnr1*<sup>fl/fl</sup> mice. Two CRISPR-Cas9 sgRNAs were used to target the upstream and downstream of exon 2 of the *Cnr1* allele, flanking the coding sequence. Three sets of primers (WT, flox, and delta) were designed for PCR detection of homologous recombination as described in Materials and Methods. (B) Validation of hepatocyte-specific *Cnr1* deletion via breeding *Cnr1*<sup>fl/fl</sup> mice with *Alb-Cre* mice. Offspring (*Hep-Cnr1*<sup>Δ/Δ</sup>) resulted in hepatic *Cnr1* deletion with the delta band and homologous recombination with flox band as identified by PCR with liver-derived and tail-derived DNA (Lower). (C) Chow-fed *Cnr1*<sup>fl/fl</sup> and *Hep-Cnr1*<sup>Δ/Δ</sup>

mice (n = 5-8/group) were euthanized at 22 weeks of age. Hypothalamus, brown adipose tissue (BAT), iWAT, gonadal white adipose tissue (gWAT) and quadriceps were collected for RNA extraction. CB-1 mRNA expression levels were quantified by real-time PCR.  $\beta$ -actin was used as an invariant control. The values were expressed relative to that of chow fed *Cnr1<sup>fl/fl</sup>* mice, which was arbitrarily set to 1. Corresponding mean CT values are denoted above. Results shown as mean  $\pm$  SEM. \*p < 0.05, \*\*p < 0.01 between genotypes, assessed by ANOVA.



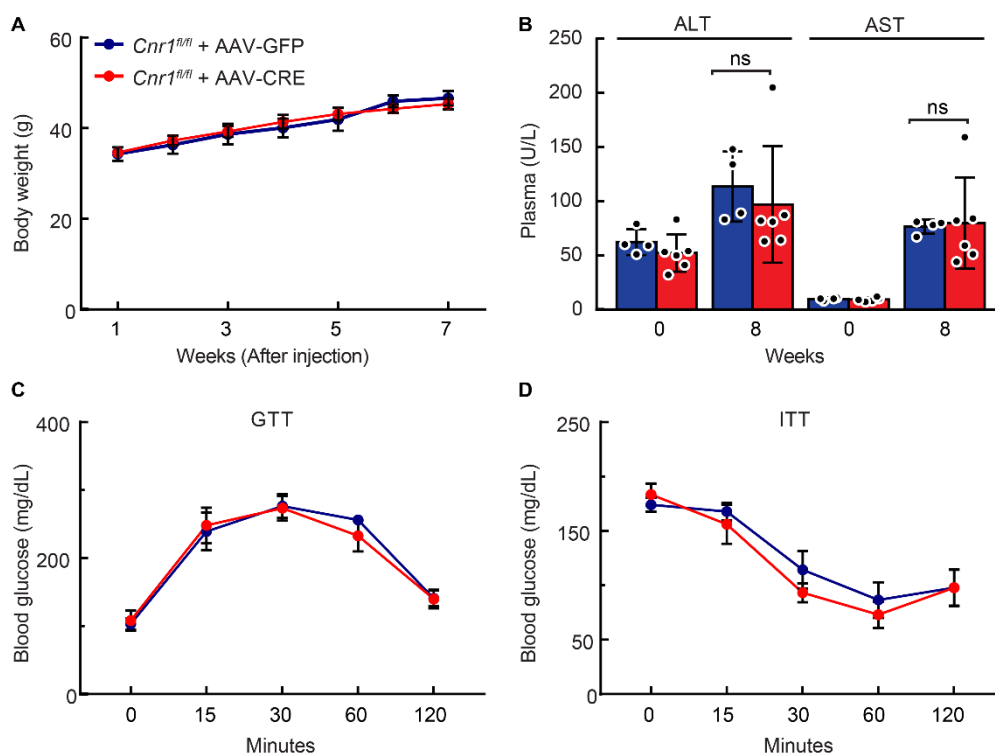
**Supplemental Figure 2. *Cnr1* deletion in hepatocytes does not affect body weight, liver function or diet-induced obesity in 16-week old mice fed chow or the HFD.** Growth curves of chow-fed (**A**) and HFD-fed (**B**)  $Cnr1^{fl/fl}$  and  $Hep-Cnr1^{-/-}$  mice (n = 5-8/group). Body weights were monitored weekly starting at 5 weeks of age. (**C**) Plasma ALT and AST levels. (**D**) Relative mRNA levels of ApoB, CB-1, Col1A1, Lrat and  $\alpha$ SMA quantified by qPCR. ApoB was used as an invariant control. Values are expressed relative to chow fed  $Cnr1^{fl/fl}$  mice, which was arbitrarily

set to 1. Corresponding mean CT values are denoted above. **(E)** Mean area of collagen was obtained by calculating the PSR-stained red area in the image under split green channel, as described in Methods. Results shown as mean  $\pm$  SEM, assessed by ANOVA. **(F)** H&E, trichrome and PSR staining of liver sections. Scale bar = 100  $\mu$ m. All experiments **(A-F)** were repeated with a separate cohort of mice and with similar results.

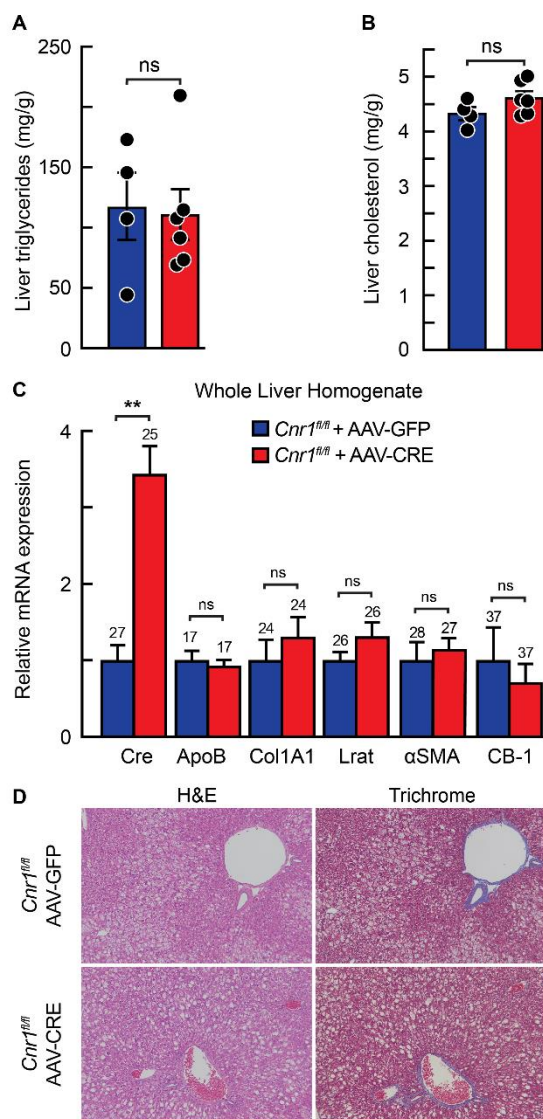


**Supplemental Figure 3. Hepatocyte-specific *Cnr1* deletion does not affect glucose tolerance, insulin sensitivity or liver steatosis in mice fed chow or the HFD.** Mice used are those described in **Supplemental Figure 2**. Glucose and insulin tolerance tests were carried out 2 and 3 weeks prior to euthanasia, respectively. (**A** and **B**) Blood glucose levels were measured at indicated times after glucose injection. (**C** and **D**) Blood glucose levels were measured at indicated times after insulin injection. (**E** and **F**) Liver TG and cholesterol levels. (**G**) Total RNA was extracted from each mouse liver, and the relative mRNA expression levels of ApoB, Srebp-1c, Srebp-2, Chrebp,

Acly, Acc1, Fasn, Scd1, and Elovl6 were quantified by real-time PCR.  $\beta$ -actin was used as an invariant control. The values were expressed relative to that of chow fed *Cnr1<sup>fl/fl</sup>* mice, which was arbitrarily set to 1. Corresponding mean CT values are denoted above. Acly, ATP-citrate lyase; Chrebp, carbohydrate response element binding protein; Elovl6, elongation of long chain fatty acids family member 6; Fasn, fatty acid synthase; Scd1, stearyl CoA desaturase 1. All experiments (**A-G**) were repeated in a separate cohort of mice with similar results.

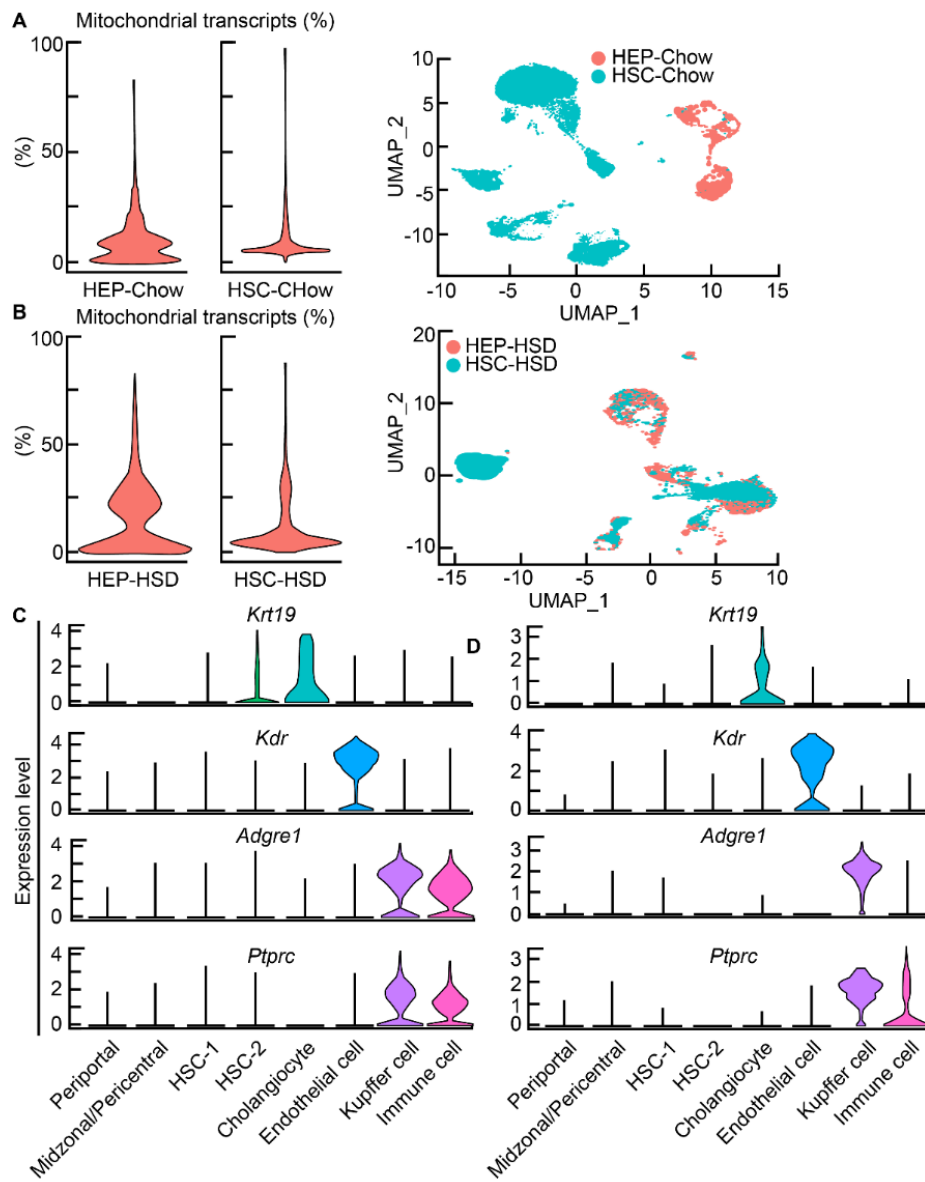


**Supplemental Figure 4. *Cnr1* deletion in hepatocytes does not alter body weights, liver function tests, or measures of insulin sensitivity in mice fed the HFD.** *Cnr1<sup>fl/fl</sup>* mice were fed a HFD for 8 weeks and then injected with control AAV-GFP or AAV-Cre (n=4-6 per group). Mice were continued on HFD for another 8 weeks. **(A)** Body weights were monitored weekly following AAV injection. **(B)** Plasma ALT and AST levels were measured before and 8 weeks after AAV injection. The glucose and insulin tolerance tests were carried out 6 and 7 weeks after AAV injection, respectively. **(C)** Blood glucose levels were measured at indicated times after glucose injection. **(D)** Blood glucose levels were measured in mice at indicated times after insulin injection.



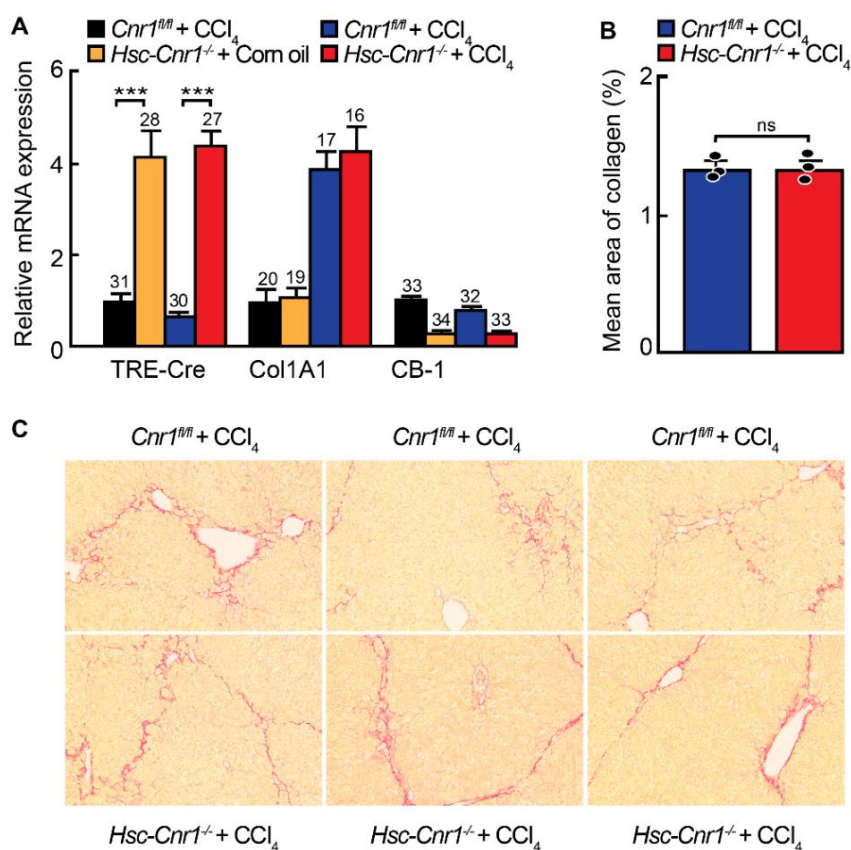
**Supplemental Figure 5. *Cnr1* deletion in hepatocytes does not reverse liver steatosis in mice fed the HFD.** The mice used here are the same as those described in **Supplemental Figure 4**. *Cnr1<sup>fl/fl</sup>* mice were fed a HFD for 8 weeks and then injected with control AAV-GFP or AAV-CRE (n=4-6 per group). The mice were continued on HFD for another 8 weeks and sacrificed for analysis. **(A)** Liver TG levels. **(B)** Liver cholesterol levels. **(C)** Real time qPCR analysis. Total RNA was extracted from each mouse liver, and the relative mRNA levels of Cre, ApoB, Col1A1, Lrat,  $\alpha$ SMA and CB-1 were quantified by real-time PCR.  $\beta$ -actin was used as an invariant control. The values were expressed relative to that in *Cnr1<sup>fl/fl</sup>* mice injected with AAV-GFP (Control)

, which was arbitrarily set to 1. Corresponding mean CT values are denoted above. **(D)** Mice were euthanized 8 weeks after AAV injection. Liver sections were processed for H&E and trichrome staining. Magnification of x20. Scale bar = 100  $\mu$ m. The same experiment was repeated in a separate cohort of mice with similar results.

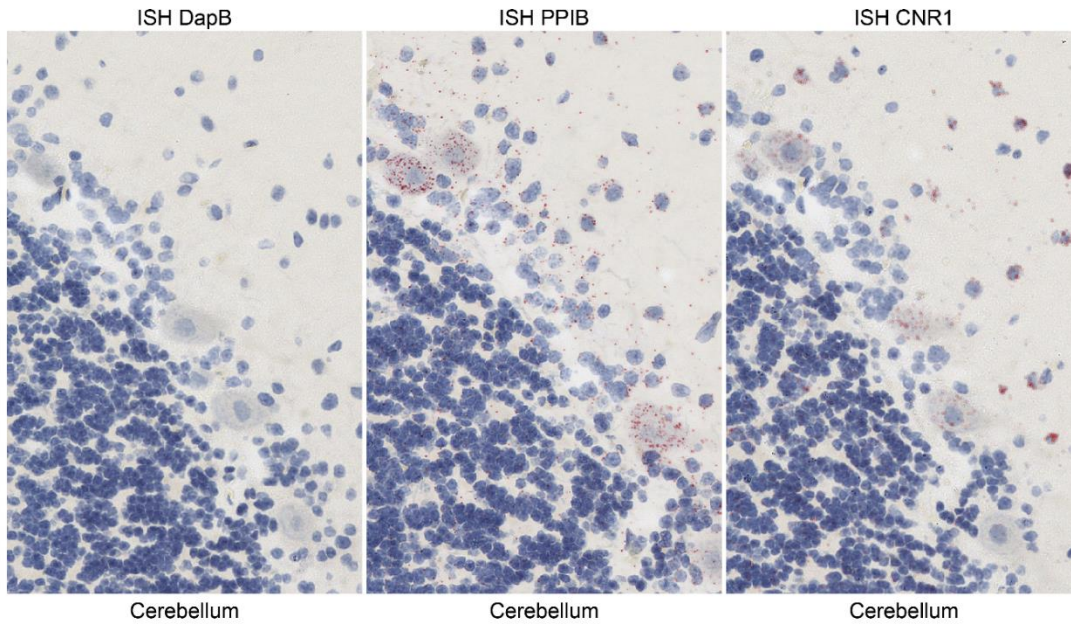


**Supplemental Figure 6. Mitochondrial transcripts and cell cluster identification.**

Mitochondrial transcript proportion in scRNA-seq data integrated from (A) chow-fed wild-type mice or (B) wild-type mice maintained on HSD for 17 weeks. Violin plots of cell type-specific signature gene expression in (C) chow-fed wild-type mice and (D) wild-type mice maintained on HSD for 17 weeks: *Krt19* (cholangiocytes), *Kdr* (endothelial cells), *Adgre1* (Kupffer cells), and *Ptprc* (immune cells).



**Supplemental Figure 7. Determination of collagen area using PSR staining.** The mice used are those described in **Figure 5**. (A) Mice used are those described in **Figure 5E**. Total RNA was extracted from HSCs, and the relative mRNA levels of TRE-Cre, Col1A1, and CB-1 were quantified by real-time PCR.  $\beta$ -actin was used as an invariant control. Values were expressed relative to that of chow-fed doxycycline-treated *Cnr1<sup>fl/fl</sup>* mice injected with corn oil, which was arbitrarily set to 1. Corresponding mean CT values are denoted above. \*\*\* $p < 0.01$ . (B) Mean area of collagen was obtained by calculating the PSR-stained red area in the image under split green channel, as described in Methods. Results shown as mean  $\pm$  SEM, assessed by ANOVA. (C) PSR staining of liver sections from chow-fed doxycycline-inducible *Cnr1<sup>fl/fl</sup>* ( $n=3$ ) and *Hsc-Cnr1<sup>-/-</sup>* ( $n=3$ ) mice injected with CCl<sub>4</sub>. Scale bar = 100  $\mu$ m. All experiments (A-C) were repeated with a separate cohort of mice and the results were similar.



**Supplemental Figure 8. CB-1 is highly enriched in human cerebellum.** Species-specific positive and negative control probes for a quality control of the automated ISH assay. Human cerebellum is used as positive control tissue for the CNR1 gene. Left panel: *Bacillus subtilis* dihydrodipicolinate reductase (DapB) gene used as non-specific bacterial negative control probe. Middle panel: Peptidylpropyl isomerase B (PPIB) housekeeping gene as species-specific positive control probe. Right panel: CNR1 detection (red punctate dot in human Purkinje cells and neurons of both the molecular and granular cell layers of the cerebellum). Scale bar = 30  $\mu\text{m}$ .

## Tables

Supplementary Table 1. Human Liver Tissue Information

Donors	Gender	Age	Ethnicity	Pathological Diagnosis	Diagnostic Information
Control					
C1	Female	44	Caucasian	Normal	Fibrosis Stage 0, NASH=1
C2	Female	67	African American	Normal	Fibrosis Stage 0, NASH=1
C3	Male	43	Caucasian	Normal	Fibrosis Stage 1, NASH=0
NAFLD/NASH					
N1	Male	3	Caucasian	NAFLD with fibrosis	Fibrosis Stage 2, NASH=2
N2	Male	58	Caucasian	NASH with fibrosis	Fibrosis Stage 2, NASH=8
N3	Female	56	Caucasian	NASH with fibrosis	Fibrosis Stage 2, NASH=6
N4	Female	57	Caucasian	NAFLD with hepatitis and fibrosis	Fibrosis Stage 2, NASH=2
N5	Female	59	Caucasian	NAFLD with hepatitis and fibrosis	Fibrosis Stage 2, NASH=1
N6	Female	46	Caucasian	NAFLD with hepatitis and fibrosis	Fibrosis Stage 2, NASH=4
N7	Female	27	African American	NAFLD with hepatitis and fibrosis	Fibrosis Stage 2, NASH=3

**Supplementary Table 2. Histological Assessment and Scoring of *In-situ* Hybridization**

Staining Distribution (D)*	Score	Staining Intensity (I)#	Score
-	0	-	0
1-25%	1	1-3	1
26-50%	2	4-25	2
51-75%	3	>25	3
76-100%	4	Many coalesced dots and not countable	4

\*staining distribution is determined by the approximate qualitative percentage of positive cells within this cell type population in the whole tissue section examined.

#staining intensity is determined by the number of dots per cell.

**Supplementary Table 3. *In-situ* Hybridization of CNR1 mRNA Expression in Human Liver Tissues**

Donors	Control			NAFLD/NASH						
	C1	C2	C3	N1	N2	N3	N4	N5	N6	N7
Probes	HsCnr1			HsCnr1						
Liver Cell Types										
Hepatocytes, centrilobular	-	-	-	-	-	-	-	-	-	-
Hepatocytes, midzonal	-	-	-	-	-	-	-	-	-	-
Hepatocytes, periportal	-	-	-	-	-	-	-	-	-	-
Cholangiocytes *	1I/1D	1I/1D	1-2I/1D	1-2I/1D	1I/1D	1I/1D	1-2I/1D	1-2I/1D	1I/1D	1I/1D
Kupffer cells <sup>#</sup>										
Stellate cells <sup>#</sup>	1I/1D	-	1I/1D	-	-	1I/1D	1I/1D	1I/1D	-	-
Sinusoidal cells <sup>#</sup>										
Vascular smooth muscle	-	-	-	-	-	-	-	-	-	-
Endothelium	1-3I/1-3D	1-2I/0-2D	1-3I/1-3D	1-2I/0-2D	1-2I/0-2D	1-2I/0-3D	1-3I/1-3D	1-2I/0-2D	1-2I/1D	1I/1D
Mononuclear cells	1I/1D	-	-	1I/1D	1-2I/1D	1I/1D	1-2I/1D	1I/1D	1-2I/1D	-

\* low positivity in large ducts.

<sup>#</sup> low abundance of CNR1 mRNA; all present at close proximity in liver parenchyma/sinusoids.